



Science Arts & Métiers (SAM)

is an open access repository that collects the work of Arts et Métiers Institute of Technology researchers and makes it freely available over the web where possible.

This is an author-deposited version published in: <https://sam.ensam.eu>
Handle ID: <http://hdl.handle.net/10985/9670>

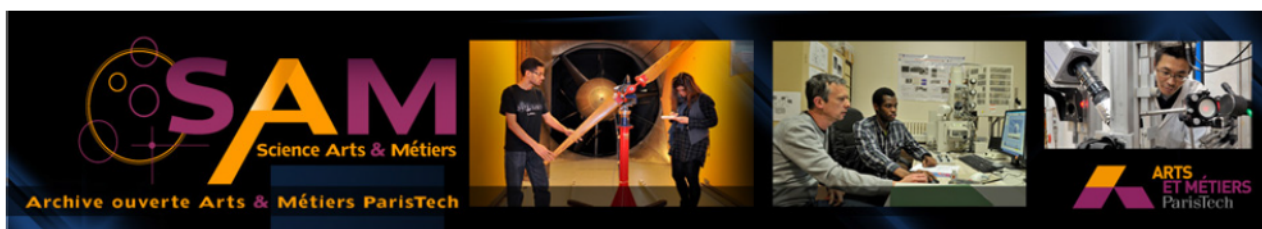
To cite this version :

Mamoun FELLAH, Mohamed LABAIZ, Omar ASSALA, Leila DEKHIL, N. ZERNIZ, Alain IOST - Tribological behavior of biomaterial for total hip prosthesis - Matériaux & Techniques - Vol. 102, p.1-8 - 2014

Any correspondence concerning this service should be sent to the repository

Administrator : scienceouverte@ensam.eu





Science Arts & Métiers (SAM)

is an open access repository that collects the work of Arts et Métiers ParisTech researchers and makes it freely available over the web where possible.

This is an author-deposited version published in: <http://sam.ensam.eu>
Handle ID: <http://hdl.handle.net/10985/9670>

To cite this version :

M. FELLAH, M. LABAÏZ, O. ASSALA, L. DEKHIL, N. ZERNIZ, A. IOST - Tribological behavior of biomaterial for total hip prosthesis - Matériaux & Techniques - Vol. 102, p.1-8 - 2014

Any correspondence concerning this service should be sent to the repository

Administrator : archiveouverte@ensam.eu

Tribological behavior of biomaterial for total hip prosthesis

M. Fellah^{1,2}, M. Labaiz¹, O. Assala¹, L. Dekhil³, N. Zerniz⁴ and A. Iost⁵

Abstract – Friction and wear plays an important role in determining the performance of biomaterials. To this end, the present research is carried out to understand the tribological behavior important biometallic alloy, Ti-6Al-4V under sliding contact. The friction and wear experiments were carried out using ball-on-disc and pin-on-disc tribometers in ambient air, under different conditions of normal applied loads (3, 6 and 10 N) and sliding speeds (1, 15 and 25 mm.s⁻¹) for 3000 m. The obtained research results revealed the lowest coefficient of friction was 0.038 at 1 mm.s⁻¹ and 3 N) while the higher value was in the range of 0.90 at 25 mm.s⁻¹ and 3 N). Results show that the specimens have similar friction and wear performance, although the sliding speed and applied loads are different. The tribomechanical wear, as evident from the observation of abrasion, adhesion and cracking, is the predominant wear mechanism.

Key words: Tribological behavior / friction coefficient / wear / biomaterial / Ti-6Al-4V

1 Introduction

The wide use of Ti materials for biomedical applications is constantly growing due to their specialized properties such as high specific strength, good mechanical properties, low elastic modulus, superior corrosion resistance, and higher biocompatibility compared with the other conventionally used metallic biomaterials [1]. These outstanding properties were a motivating force for the early offering of (α) cp and ($\alpha + \beta$) Titanium alloys. Ti-6Al-4V alloys as well as for the more recent development of Ti-alloy compositions of α , $\alpha + \beta$, β and metastable β Ti alloys. One of the main concerns for further development of Ti alloys for biomedical applications is undoubtedly its fretting and sliding wear resistance, when they are subjected to action of sliding and rubbing contact of articulating surfaces during their service in the body [2]. Generally, wear property can be defined as damage to a solid surface, involving progressive loss of material, due to relative motion between that surface and a contacting substance or substances. Recently main concern, for further development of biometallic implant materials, is, among others, stress transmission between hard tissue and biometallic components which are in

contact since further bone degradation and bone adsorption should be avoided [3, 4]. Namely, great difference between bone and biometallic implant materials rigidity and other mechanical and tribological characteristics may lead to further bone loss and degradation. Fretting and sliding wear conditions lead to damage and then fracture of the passive oxide film [5–8] which could be disrupted at very low shear stresses [9]. Unfortunately, Ti is an extremely reactive metal and has a reputation for poor tribological properties [10, 11] and inferior performance when compared with other implantable. In general, the friction, wear and corrosion failures are the main reasons of degradation [12] and great difference of tribological characteristics between bone and implant must be limited to increase the service life of the surgical implants and to avoid bone degradation and adsorption [4]. The poor tribological properties of Ti alloys, attributed to their low resistance to plastic shearing and low mechanical stability of the passive surface oxide layer, are significant clinical problems [13–18] which may lead to the premature removal of the prostheses. Therefore, it is of great interest to enhance the surface friction and wear resistance of orthopedic Ti alloys inside the human body that will increase the longevity

¹ Surface Engineering and Tribology Group, Laboratory of Metallurgy and Engineering Materials, BADJI Mokhtar-Annaba University, P.O. 12, 23000 Annaba, Algeria
mamoun.fellah@yahoo.fr

² Mechanical Engineering Department, ABBES Laghrou, Khenchela University, P.O 1252, 40004 Khenchela, Algeria

³ Laboratory of formability of materials BADJI Mokhtar, Annaba University, P.O. 12, 23000 Annaba, Algeria

⁴ Laboratory of Inorganic Materials Chemistry BADJI Mokhtar, Annaba University, P.O. 12, 23000 Annaba, Algeria

⁵ ARTS ET METIERS ParisTech, MSMP, 8 Boulevard Louis XIV, 59046 Lille Cedex, France

Table 1. Chemical composition, hardness and microstructure of the metallic material studied.

Ti	C	Mo	Ta	Fe	Al	Nb	V
Bal	0.03	0.01	–	0.10	6.7	–	4.2
Hardness: 360 ± 10 HV		Microstructure: 80% α 20% β					

of total joint components. Much research efforts have been devoted to study and improve the performance in terms of the wear behavior of the biomedical Ti alloys. Various proper surface modification techniques, such as ion implantation, TiN coating, thermal oxidation, composition adjustment and selection of appropriate thermal and thermomechanical processing procedures have thus been proposed to improve the wear resistance by changing the nature of the surface [19–21]. The aim of the present study was to study the friction and wear behavior of Ti6Al4V alloy under different condition of applied load and sliding speed. The tests were carried out under dry sliding conditions against a 100Cr6 “counter material”.

2 Materials and methods

2.1 Materials characterization

The material used in this study is the Ti-6Al-4V as a total hip prosthesis (femoral stem), that was cut from a titanium cylindrical bar corresponding to ISO 5832-3 part 3/ 01-07-199 (supplied by ENSAM Lille, France). The chemical composition of titanium alloys used in this study is specified in Table 1.

The alloy surfaces were ground with 600 SiC abrasive papers and polished with colloidal silica since it is known that the fixation of the implant is greatly dependent on good mechanical interlocking between the rough surface of the implant and tissue [22]. All the samples were cleaned in an ultrasonic bath with acetone, ethanol, and distilled water, for 10 min in succession and then dried in hot air and saved in the dessicator till their use.

2.1.1 Surface and microstructural analysis

After etching by a solution of 3 ml HF, 6 ml HNO₃ and 100 ml H₂O for 10 s to reduce the influence of surface hardening, the microstructure was studied using optical microscopy (Leica DMLM). The alloys chemicals composition presented in Table 1 was acquired using spectrometer (Spectrolab) and energy-dispersive spectroscopy (EDS using PHILIPS XL 30 ESEM-FEG, and EDX IMIX-PTS). The phases presented in alloy microstructure were identified by X-Ray Diffractometry (Intel CPS 120/Brucker AXS) using Cu K α generated at 40 kV and 35 mA. Scanning electron microscopy (SEM) and energy dispersive X-ray (EDX) analyses were used to study the chemical composition of investigated materials. The roughness of the samples in 3D was studied using Surface Data Veeco: Mag 50 X, VSI mode.

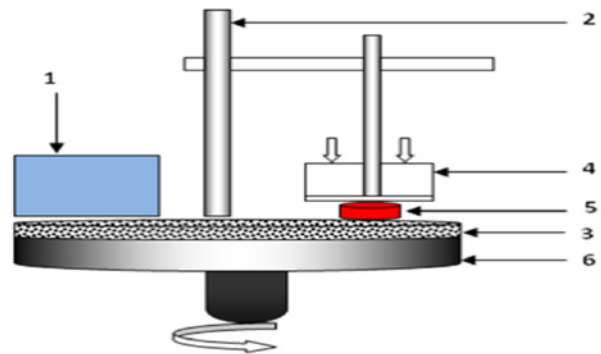


Fig. 1. Scheme of pin on disc system: 1 – Speed regulator, 2 – support, 3 – Rotating tray, 4 – load applied, 5 – Sample, 6 – retaining frame.

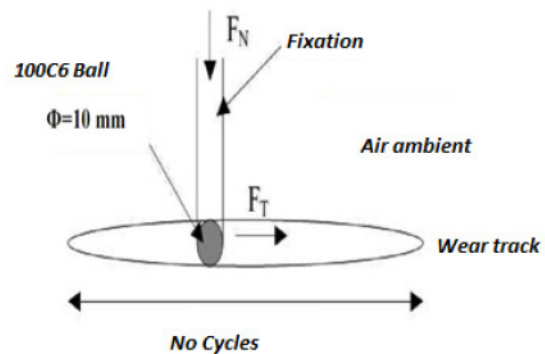


Fig. 2. Scheme of ball on disc contact (alternative movement).

2.2 Tribological study

Pin on disc, ball on disc and tribological tests (Figs. 1 and 2) were carried out using the following prosthetic materials: Ti-6Al-4V alloys, against 100Cr6 steel and abrasive Sic paper grade 320.

2.2.1 Weight loss: (Pin on disc)

The contact pair, used to study the weight loss is the sample and the 320 abrasive paper. The parameters taken into account for this test are the applied load (3.5 N) and the rotational speed.

The test time and sliding distance (1300 m) are kept constant, while the weight loss is determined as a the difference in the weight of the sample before and after the test. A microelectronic balance, whose accuracy is of the order 10^{-3} g, was used for weight measurements. The samples were cleaned with acetone before each weight and the surface roughness of the test sample is measured before and after the test.

2.2.2 Friction and wear behavior (Ball on disc)

Experiments tests have been carried out, in ambient air with an oscillating tribometer in accordance with

Table 2. Work condition of alternative movement wear test.

Friction pairs used	100Cr6 steel/Ti-6Al-4V
Sliding speed	1, 15 and 25 mm.s ⁻¹
Applied load (N)	3, 6 and 10 N
Wear track radius	5 mm
100Cr6 steel diameter	10 mm
Temperature	25 °C
Humidity	38%

ISO 7148, ASTM G99-95a and ASTM G133-95 standards (Fig. 2) Samples were prepared for testing in accordance with ASTM F136-02, ASTM F86-01, ASTM E1078-02. Each specimen was thoroughly cleaned by ethyl alcohol, then cleaned in ultrasonic bath for 60 min and dried in hot air afterwards. After that, samples were cleaned in isopropyl alcohol, by staying in the solution for 60 min and dried in a hot air. Samples were stored in dessicator, prior to testing. Duration of each test was 4000 m (distance of 300 m), whereat one cycle is represented by full amplitude sliding distance (half amplitude, 0.25 mm). Selected sliding velocities lie in the range typically found in hip joints (1, 15 and 25 mm.s⁻¹) under different normal loads (3, 6 and 10 N). The friction coefficient, i.e. dynamic friction coefficient, was automatically recorded during the testing, using data acquisition software. Simultaneously, the friction coefficient curve was recorded and plotted. Test conditions are shown in Table 2.

3 Results

3.1 Surface and microstructural analysis

Samples of the titanium based alloys (Fig. 3) were examined using (EDX) analysis. The spectra for the overall analysis are shown in Figures 4 and 5. In the case of Ti-6Al-4V alloy titanium, Ti peak is more pronounced than aluminum as expected in the EDX phases. Vanadium, molybdenum (Mo), nickel is also present. The chemical compositions of the studied sample in accordance with that of a Ti-6Al-4V.

3.1.1 Microstructure

Alloy microstructure (Fig. 3) consist of globular and acicular α grains (white grains) within a matrix containing equiaxial β grains (dark grains). The acicular shape of the α phase is present in the Figure 3 in an arrangement known as basket-weave which characterizes the Widmanstätten structure.

3.1.2 Microhardness

Microhardness experiments (Fig. 6) were performed using universal hardness testing machine type ZHU/Z 2.5, equipped with a Vickers diamond indenter, located

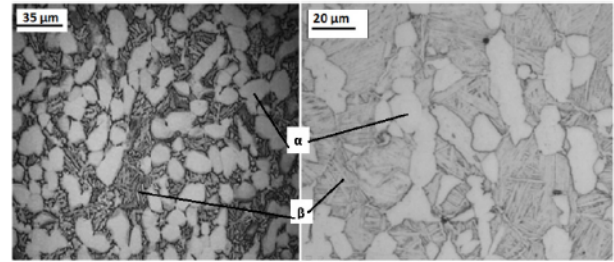


Fig. 3. Optical micrographs of Ti-6Al-4V alloys.

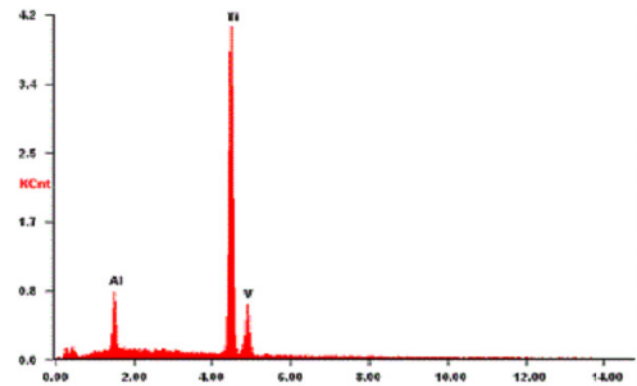


Fig. 4. EDX spectrum of Ti-6Al-4V alloy.

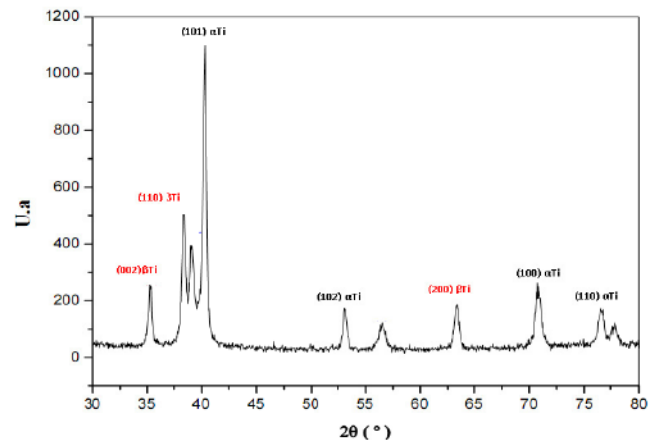


Fig. 5. XRD spectrum of Ti-6Al-4V alloy.

in a room temperature of 22 °C and atmosphere of laboratory. Using the P-h load-penetration curves during micro hardness experiments with a 0.2 mm.min⁻¹ loading speed; under a maximum load of 50 N, each test was conducted three times, and the average values were calculated automatically.

3.1.3 Roughness analysis

The studied substrates are of biomedical interest. They must therefore meet the standards imposed by the field of biomedicine particularly at the surface of the material deposited on the articular surfaces of hip prostheses in which Ti-6Al-4V is the hip implant. The obtained

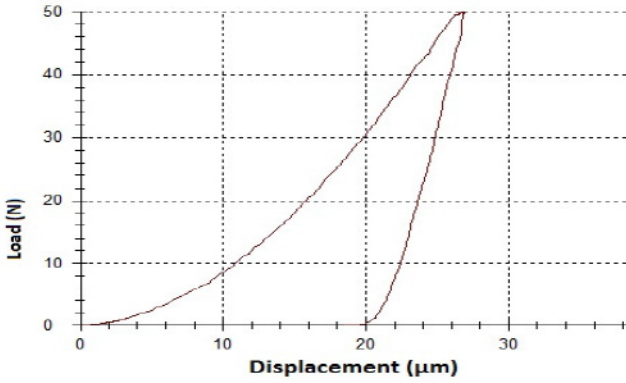


Fig. 6. P-h curves during micro hardness experiments.

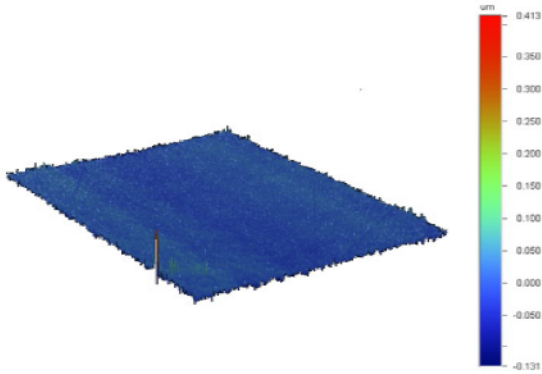


Fig. 7. Optical 3D photos of Ti-6Al-4V after polishing.

Table 3. Roughness parameters of Ti alloy after polishing.

Parameters	R_a	R_q	R_z	R_t
(μm)	0.02	0.08	1.05	1.19

R_a : arithmetic average of absolute values, R_q : root mean squared, R_t : maximum height of the profile and R_z is the average distance between the highest peak and lowest valley in each sampling length.

roughness of the samples (Tab. 3 and Fig. 7), meets the standards of biomedicine, as specified in ISO 7206-2:1996 standard [23]. The roughness values R_a were 6.03 and $0.02 \mu\text{m}$ for Ti-6Al-4V alloy before and after polishing, respectively.

3.2 Tribological study

3.2.1 Weight loss (contact plane)

The weight loss (Fig. 8) of titanium samples, tested at 3.5 N load, is approximately proportional to the number of disc revolutions. Nevertheless, the wear was systematically greater to ceramic (α -alumina) as expected in Figure 8. The behavior observed for both samples suggests that the wear mechanism during the test is the same (abrasive wear). In the case of Ti-6Al-4V samples, its

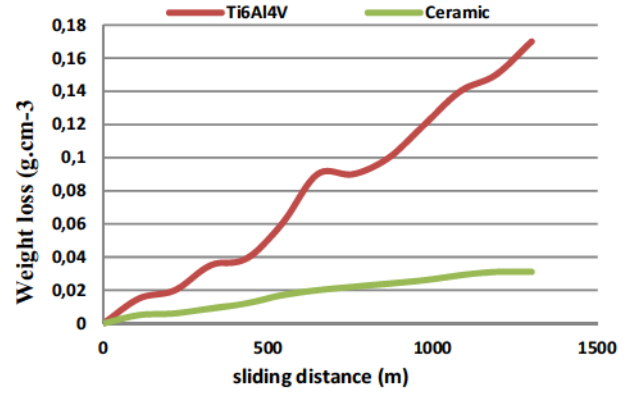


Fig. 8. Weight loss of Ti6Al4V alloys during wear sliding against abrasive paper.

weight loss was $\sim 85\%$ of the one observed for the ceramic samples.

According to the Archard's law, the volumetric loss of the material is inversely proportional to the hardness value of the material [24, 25]. This implies that the higher the hardness of the material, the smaller is the volume loss. The present alloys exhibit significant difference in hardness values, so that the experimental sliding wear data correlate well with Archard's law.

3.2.2 Friction coefficient

Dependence of Ti-6Al-4V alloys coefficient of friction (COF) on sliding distance, i.e. number of cycles, is given in Table 4 and from Figures 9–11, are almost the same form wholes in terms of load and speed. The analysis of these curves permits to distinguish several periods or successive regimes of friction and wear:

1. The first is accommodation period, during which the friction coefficient increases rapidly, it is the surface of the first body (the most ductile) [26]. The roughness of the sample surface is reduced by plastic deformation.
2. The second period is characterized by a slight decrease in the friction coefficient. Probably, the third body on the track generated by frictional wear of the steel plays a role comparable to that of a solid lubricant.
3. The third and final period corresponds to the stabilization of the friction coefficient up 1300 m.

It is seen from Figures 10–12, that the friction coefficient displays a lower value (approx. 0.248) up to 20 m and then increases up to the average 0.4 value between 40 and 1000 m. The reason might be due to oxide layer formed on titanium alloys and, therefore, the coefficient of friction showed the lower value. However, that oxide layer was torn and then 100Cr6 steel ball was completely touched on the titanium alloy and, therefore, the friction coefficient reached a higher value (0.538).

Figures 10 and 11 displays the evolution of friction coefficient curves of Ti-6Al-4V, under different condition of applied loads, and sliding speeds ($1, 15$ and $25 \text{ mm}\cdot\text{s}^{-1}$). The results obtained showed the same form for all curves.

Table 4. Friction coefficient of Ti-6Al-4V alloy under different condition of applied loads and sliding speeds.

Speed mm.s^{-1}	Load N	COF _{Start}	COF _{Min}	COF _{Max}	COF _{Mean}
1	3	0.158	0.038	0.521	0.356
	6	0.064	0.058	0.498	0.297
	10	0.23	0.217	0.54	0.374
15	3	0.229	0.229	0.809	0.597
	6	0.406	0.351	0.659	0.473
	10	0.308	0.308	0.607	0.452
25	3	0.193	0.193	0.754	0.489
	6	0.355	0.355	0.904	0.565
	10	0.372	0.349	0.648	0.476

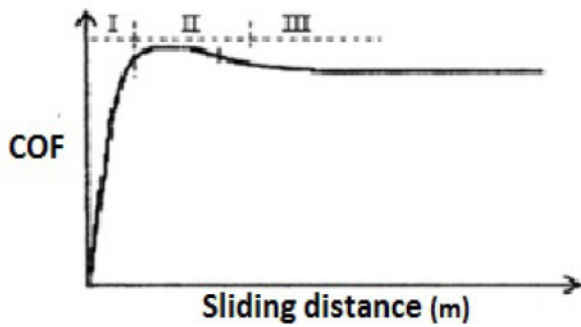


Fig. 9. Different periods distinguished in friction curves.

A. Influence of load

Table 4 and Figure 10 represent the influence of applied load on the evolution of friction coefficient, under different conditions of loads and sliding speeds. It is seen in the Figure 10a at 1 mm.s^{-1} , that the Ti-6Al-4V displayed a lower value at 6 N up 500 m, compared to the 3 N and 10 N. The results presented in Figures 10b and 10c show that the coefficient of friction almost has the convergent value under investigated conditions.

The results show in Figure 10b that the average friction coefficients were 0.59, 0.473 and 0.452 for the Ti-6Al-4V alloy, at normal loads 3 N, 6 N and 10 N respectively. It is also obvious that the coefficient of friction displayed a lower value (0.229, 0.351 and 0.308) up to 100 m for the Ti-6Al-4V and then it sharply increased to the average value of 0.809, until 2300 distance (m) distance.

It is seen in Figure 10c, that the Ti-6Al-4V has higher values of friction coefficient (0.754, 0.904 and 0.648). It is also obvious, that the coefficient of friction displayed a lower value at 0.193 and 0.349, up to 50 m, and then it sharply increased to the average value of 0.75 until 1400 m.

Figure 11 represents the influence of applied load to the evolution of the friction coefficient of Ti-6Al-4V alloy under different loads and sliding speeds. It is seen that, the mean coefficient of samples displayed a lower value at 1 mm.s^{-1} , and then it sharply increased to the average value with increasing of sliding speed as shown in Figure 12.

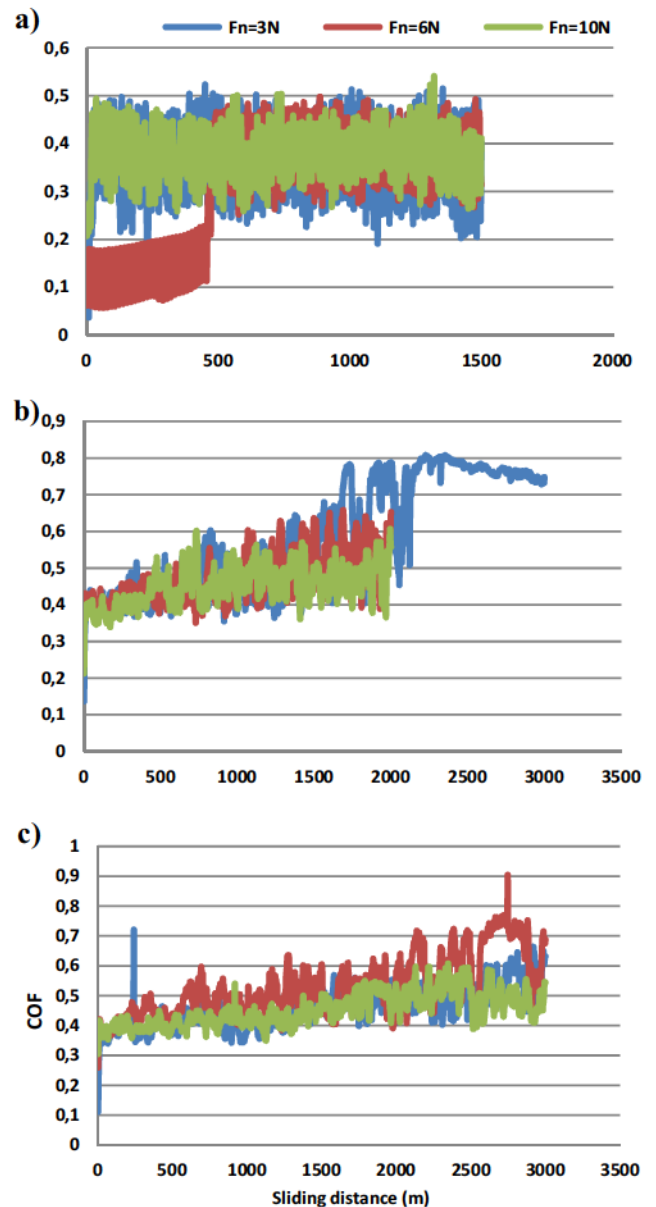


Fig. 10. Friction coefficient of titanium alloys versus sliding distance under different conditions of loads at: (a) 1 mm.s^{-1} , (b) 15 mm.s^{-1} and (c) 25 mm.s^{-1} .

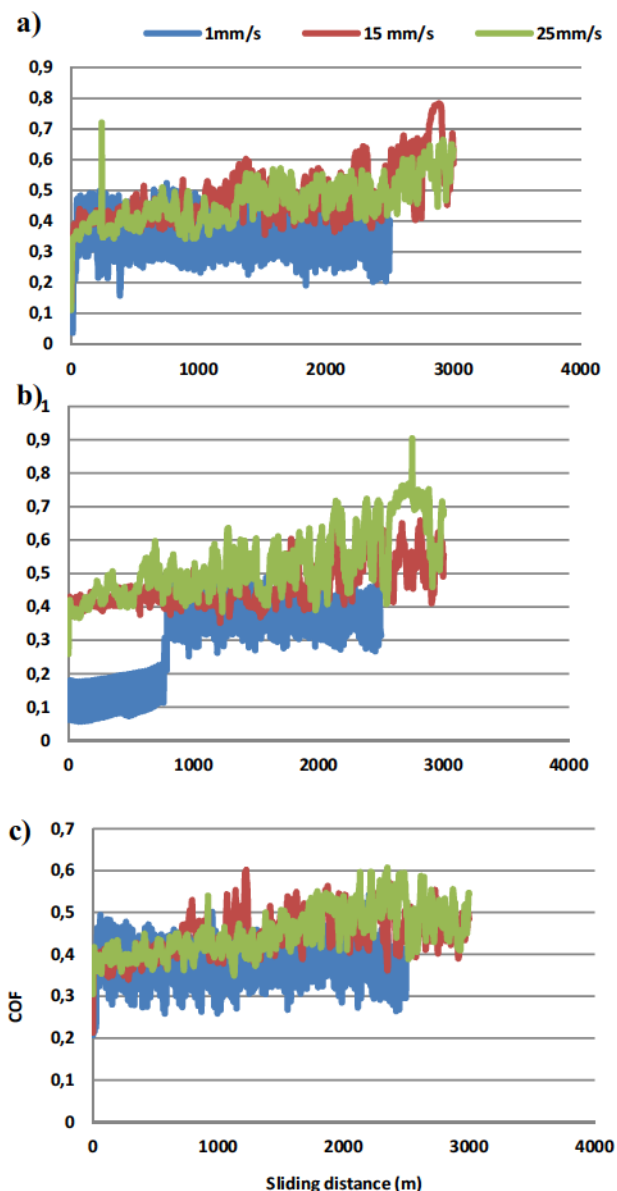


Fig. 11. Friction coefficient of titanium alloys versus sliding distance under different sliding speeds at: (a) 3 N, (b) 6 N and (c) 10 N.

B. Influence of speed

3.2.3 Wear behavior

The volumetric wear rate (Fig. 13) was calculated using the mechanical profilometre surfest SJ-301. A 100Cr6 steel ball did the grinding from the sample surface, that is, abrasive wear occurred on the surface and is illustrated in Figures 12 and 13. Volumetric wear was determined as 5.45×10^{-3} , 9.53×10^{-3} and $12.08 \times 10^{-3} \text{ mm}^3 \text{ N}^{-1} \text{ mm}^{-1}$ for the Ti-6Al-4V at 1 mm.s^{-1} sliding speed under load 3, 6 and 10 N respectively. Finally, the volumetric wear was the same (convergent values) for both sliding speed 15 and 25 mm.s^{-1} between 22.35×10^{-3} and $54.21 \times 10^{-3} \text{ mm}^3 \text{ N}^{-1} \text{ mm}^{-1}$ for both samples. Figure 13

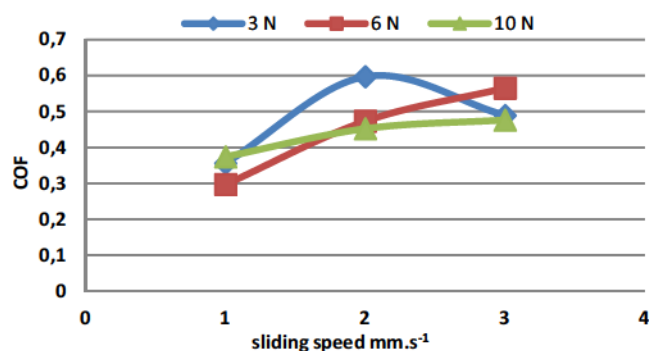


Fig. 12. Mean coefficient of friction of titanium alloys under different conditions of loads and sliding speeds.

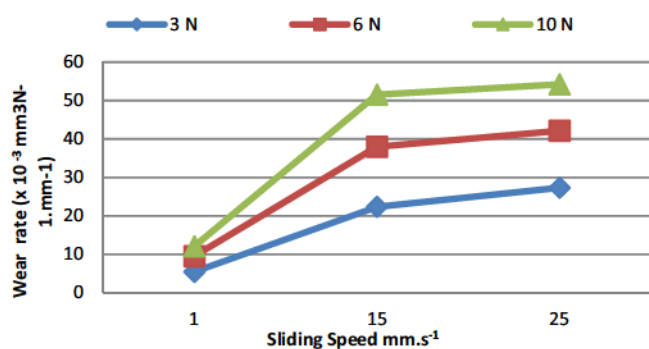


Fig. 13. Wear rate ($\text{mm}^3 \text{ N}^{-1} \text{ mm}^{-1}$) Ti-6Al-4V under different conditions.

provides the wear volume of the investigated alloy as a function of the sliding speed. The volumetric wear data reveal that the volume loss, increases as the sliding speed increases.

4 Discussion

4.1 Friction behavior

The results of the hardness testing show that Ti-6Al-4V alloy is characterized with high hardness. Dependence between wear characteristics and hardness was reported earlier and wear value decreased with hardness increase [27]. When the properties of titanium alloy were evaluated by parameters obtained from indentation depth, depth was found to decrease with increasing content of impurities [27]. The change in depth value is caused by the effect of yield strength [28] and flow stress [29]. The differences in weight loss (Fig. 8) and worn surface characteristics among the two metals can be partially attributed to the differences in hardness and the deformation process associated with microstructural characteristics. In addition, there are other factors which influence material wear characteristics. Wear particles have an influence by a surface-damage mechanism [30], and the surface condition was reported to be influential in the wear characteristics of biomaterials alloys [31]. In order to identify phase constitution, titanium alloys were

subjected to X-ray diffraction analysis using $\text{CuK}\alpha$ radiation. Presence of both α and β phases was confirmed, and mostly the peaks corresponding to the α phase (hexagonal closed packed) and β phase (body-centered cubic) appeared [32, 33]. Microstructure of the Ti-6Al-4V alloy exhibits α refined two-phase structure consisting of acicular α phase in prior- β grains. Strength of the alloy is considered to stem from this refined structure.

4.2 Wear behavior

Figure 13 provides the wear volume losses of the investigated alloys as a function of the sliding speed. The volumetric wear data reveal that the volume loss, increases as the sliding speed increases.

At higher sliding speeds, the difference in wear loss is even much higher. This can be explained by the fact that as sliding speed increases, the oxidative wear decreases because of the reduction of the time available for the out-of-contact oxidation [34]. The oxidative wear is characterized by the formation of surface oxide islands which are continuously formed and worn away. If the oxide scales on the worn surface are not sufficiently supported by the underlying strain-hardened material and do not adhere to the substrate, they tend to be continuously fragmented. Therefore, they are not protective and the resulting wear is severe. Since the surface of fixed specimens in the present investigation is under continuous contact, one of the reasons for poor wear resistance of investigated alloys is their inability to form protective oxide layer during wear.

The morphological analysis of the wear tracks confirms the above results. The SEM micrographs presented in Figure 14 show the typical worn surface morphologies of the specimens tested at the lowest and highest sliding speed. The morphologies of the specimens worn at the intermediate sliding speed are not shown because they show intermediate characteristics between these two extremes. On the worn surfaces of both alloys, evidences of abrasion wear can be detected in all tested specimens.

Continuous sliding marks with plastically deformed grooves and ridges are seen on the wear tracks independently of the sliding speed. However, the extent of plastic deformation or “ploughing” is found to be smaller. Layers with consistent plastic deformations are relatively smooth at all evaluated speeds (Fig. 14). Only the shallow wear grooves resulted from the penetrating of hard rigid abrasives and subsequent scratching of the specimen surface by the penetrated abrasives can be observed. The penetration depth depends on the relative hardness of the abrasive with respect to the specimen surface hardness.

The SEM examination also shows that at least two wear mechanisms are operative in the Ti-6Al-4V. Existence of the flakes removed from the contact surface by delamination of material strongly suggests the occurrence of adhesive wear. During sliding, the contacting asperities experience an incremental plastic deformation, which accumulates during repeated contacts [35].

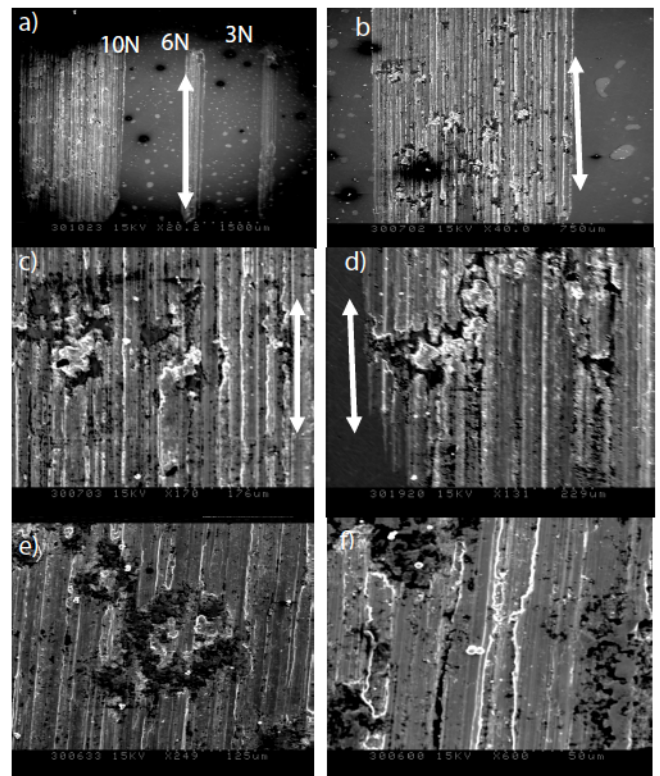


Fig. 14. SEM micrographs of alternative wear marks on Ti-6Al-4V sample after the friction test at $15 \text{ mm}\cdot\text{s}^{-1}$, (a) 3 N, (b) 6 N (c) 10 N and $25 \text{ mm}\cdot\text{s}^{-1}$, (d) 3 N, (e) 6 N, (f) 10 N (severe deformation and plastic flow). Arrows indicate the sliding direction.

When a critical value of the accumulated plastic strain is attained, cracks nucleate below the surface and propagate parallel to the surface. As a consequence, flakes of material are detached from the surface by adhesion to the counterpart. Some of transferred material is lost, but some is re-embedded and smeared over the contact surface. In this theory of delamination [35], successively discussed and implemented by numerous authors, it is supposed that a critical plastic strain is given by the ductility of the material. Titanium and its alloys are chemically active and have a high ductility, giving rise to the strong tendency to adhesion [36].

SEM micrographs presented in Figure 14 show the worn surfaces of Ti-6Al-4V alloy. It is evident that fracture on a much larger scale is occurred and that large flakes are removed from the surface. Detailed investigation of delaminated regions reveals ridges and cracks perpendicular to the sliding direction. Smeared areas can also be easily detected on the worn surfaces. These features indicate that the wear occurs predominantly by adhesion. In this case, the adhesion overlaps the abrasion and accelerates the wear of the Ti-6Al-4V alloy. Occurrence of delamination is more prominent when wear tests are carried out at higher sliding speeds (Figs. 14e and 14f). The same behavior was observed by Fella et al. [37].

5 Conclusions

The effects of friction and wear variables such as sliding speed, applied normal load, and sliding distance have been evaluated. The following conclusions are drawn based on the experimental investigations.

1. It was found from the SEM images that at low applied normal load the wear track indicates a micro fragmentation process, and on the other hand at high applied normal load the brittle detachment of large particles from the surface is clearly seen.
2. Large frictional fluctuations occurred, probably as a result of formation and periodic, localized fracture of a transfer layer.
3. Higher friction coefficient with more distinct value fluctuation and higher wear rate were observed at the higher sliding speed.
4. Under all investigated conditions, the friction coefficient firstly decreases and then increases as a function of the sliding distance. The evolution of the friction coefficient is related to the composition of the worn surfaces.
5. The Ti-6Al-4V alloy wear mechanism transforms from ploughing and peeling off wear at low sliding speeds to plastic deformation and adhesive wear at elevated speed.
6. The tribomechanical wear, as evident from the observation of abrasion, adhesion and cracking, is the predominant wear mechanism.
7. The observed cracking on the worn surface can be related to the heavy deformation and formation of persistent slip bands.

Acknowledgements. This work was realized in collaboration with the mechanical laboratory of MSMP Lille in France.

References

- [1] D.F. Williams, Titanium for Medical Applications. In: (Eds.) D.M. Brunette, P. Tengvall, M. Textor, P. Thomsen, Titanium in Medicine, Springer, New York, 2001
- [2] D.M. Brunette, P. Tengvall, M. Textor, et al., Titanium in medicine, Springer, Heidelberg, New York, 2001
- [3] M. Niinomi, T. Hattori, S. Niwa, Material Characteristics and Biocompatibility of Low Rigidity Titanium Alloys for Biomedical Applications, in: M.J. Yaszemski, et al. (Eds.) D.L. Wise, Biomaterials in Orthopedics, Marcel Dekker Inc., New York, 2004, pp. 41-91
- [4] L. Capitanu, J. Onisoru, A. Iarovici, et al., *Tribol. Ind.* **30** (2008) 23-32
- [5] S.A. Brown, P.J. Hughes, K. Merrit, *J. Orthopaedic Res.* **6** (1988) 572-579
- [6] D.W. Hoepfner, V. Chandrasekaran, *Wear* **173** (1994) 189-197
- [7] L.M. Rabbe, J. Rieu, A. Lopez, et al., *Clinical Mater.* **15** (1994) 221-226
- [8] M.H. Zhu, Z.B. Cai, W. Li, et al., *Tribol. Int.* **42** (2009) 1360-1364,
- [9] P.A. Lilley, P.S. Walker, G.W. Blunn, Wear of titanium by soft tissue, in: Transactions of the 4th World Biomaterials Congress, Berlin, 1992, pp. 227-230
- [10] S. Fayeulle, *Wear* **107** (1986) 61-70
- [11] I.J. Polmear, Light Alloys, Arnold, London, 1981
- [12] F. Yildiz, A.F. Yetim, A. Alsaran, et al., *Wear* **267** (2009) 695-701
- [13] M. Fellah, M. Labaiz, O. Assala, et al., *Adv. Tribol.* **2014** (2014) 13, DOI: [10.1155/2014/451387](https://doi.org/10.1155/2014/451387)
- [14] M. Geetha, A.K. Singh, R. Asokamani, et al., *Prog. Mater. Sci.* **54** (2009) 397-425
- [15] A. Choubey, B. Basu, R. Balasubramaniam, *Mater. Sci. Eng. A* **379** (2004) 234-239
- [16] Y.L. Hao, M. Niinomi, D. Kuroda, et al., *Metall. Mater. Trans. A* **33** (2002) 3137-3144
- [17] M. Fellah, O. Assala, M. Labaiz, et al., TMS 2014 Supplemental Proceedings, John Wiley & Sons, Inc., Hoboken, NJ, USA. [10.1002/9781118889879.ch32](https://doi.org/10.1002/9781118889879.ch32)
- [18] M. Fellah, O. Assala, M. Labaiz, et al., *J. Biomaterials Nanobiotechnol.* **4** (2013) 374-384
- [19] M. Niinomi, *Mater. Sci. Eng. A* **243** (1998) 231-236
- [20] G. Manivasagam, U.K. Mudali, et al., *Corros. Rev.* **21** (2003) 125
- [21] S.J. Li, R. Yang, S. Li, et al., *Wear* **257** (2004) 869-876
- [22] E. Confortoa, B.-O. Aronssonb, A. Salitoc, et al., *Mater. Sci. Eng. C* **24** 611-618 (2004)
- [23] Implants chirurgicaux – Prothèses partielles et totales de l'articulation de la hanche – Partie 2 : Surfaces articulaires constituées de matériaux métalliques, céramiques et plastiques, Norme internationale ISO 7206-2:1996(F)
- [24] J.F. Archard, *J. Appl. Phys.* **24** (1953) 981-988
- [25] M. Fellah, O. Assala, M. Labaiz, et al., *Adv. Bioceram. Porous Ceram.* **VI** (2014) 45-57
- [26] L. Avril, Elaboration de revêtements sur acier inoxydable simulation de la fusion par irradiation laser caractérisation structurale, mécanique et tribologique, thèse, ENSAM (No. d'ordre: 2003-16)
- [27] T. Yoneyama, H. Doi, E. Kobayashi, et al., *Dent Japan* **33** (1997) 92-96
- [28] A.G. Atkins, D. Tabor, *J. Mech. Phys. Solids* **13** (1965) 149-64
- [29] G. Sundararajan, Y. Tirupataiah, *Bull. Mater. Sci.* **17** (1994) 747-770
- [30] R.A. Buchanan, E.D. Rigney Jr., J.M. Williams, *J. Biomed. Mater. Res.* **21** (1987) 367-77
- [31] A.U. Yap, L.F. Ong, S.H. Teoh, et al., *J. Oral Rehab.* **26** 228-235 (1999)
- [32] H. Doi, T. Yoneyama, E. Kobayashi, et al., *J. Jpn Soc. Dent. Mater. Dev.* **17** 247-5 (1998)
- [33] D. Iijima, T. Yoneyama, H. Doi, et al., *Biomaterials* **24** (2003) 1519-1524
- [34] G. Straffelini, A. Molinari, *Wear* **236** (1999) 328-338
- [35] N.P. Suh, Update on the delamination theory of wear, in: D.A. Rigney (Ed.), Fundamentals of Friction and Wear of Materials, ASM, Materials Park, OH, 1980, p. 43
- [36] H. Dong, T. Bell, *Wear* **238** (2000) 131-137
- [37] M. Fellah, O. Assala, M. Labaiz, et al., *Tribol. Mater. Surfaces Interfaces* **7** (2013) 135-149